LETTER

Depinning field of domain walls with a misaligned grain boundary in iron-based soft magnets

Applied Physics Express **9**, 053003 (2016)
http://doi.org/10.7567/APEX.9.053003

Depinning field of domain walls with a misaligned grain boundary in iron-based soft magnets

Keisuke Yamada*†, Shota Irie, Soh Murayama, and Yoshinobu Nakatani

Graduate School of Informatics and Engineering, University of Electro-Communications, Chofu, Tokyo 182-8585, Japan

*E-mail: yamada_k@gifu-u.ac.jp
†Present address: Department of Chemistry and Biomolecular Science, Faculty of Engineering, Gifu University, Gifu 501-1193, Japan

Received March 8, 2016; accepted March 24, 2016; published online April 14, 2016

We report on the domain wall (DW) depinning in an iron-based soft magnet with a misaligned grain boundary (GB) using micromagnetic simulations. The results show that the depinning magnetic field decreases with increasing roughness of the misaligned GB. This effect can be explained from the ratio of the overlapping areas of the GB to the DW when the DW is depinned from the GB. The results presented here offer a promising route to the design of soft magnets to decrease coercive force.

Soft magnetic materials are widely used in the iron core of devices such as transformers, generators, and motors. In each device, a reduction in energy associated with electric–magnetic conversion is an issue. To achieve a reduction in energy, soft magnetic materials with low coercivity, high permeability, and low iron loss are in demand. Iron-based soft magnetic materials have been actively studied because these materials have high permeability and high saturation magnetization (i.e., low coercivity).[1–7] In these magnets, there is a grain boundary (GB) between the particles, and the magnetic domain wall (DW) motion is pinned at the GB, which is one of the origins of the coercive force in the magnets.[6,7] In a 6.5 wt% Si–Fe material (which is a nonmagnetostrictive material),[8,9] the motion of the 90° DW was measured and the pinning of the 90° DW at the GB determined the magnitude of the coercive force.[6,7] However, there are no detailed reports on the 90° DW motion at the GB. The clarification of the DW motion at the GB is key to obtaining a low coercive force in a soft magnet.

The low coercive force can change the material in the GB and the shape of the GB.[10–17] In these studies, the effect of the DW pinning on hard magnetic materials has been analyzed experimentally for several decades. The DW depinning field (H^{depin}) in hard magnets [where the DW width (δ_{w}) < the GB width (γ_{w})] is as follows:[10–12]

$$H^{\mathrm{depin}} = \frac{2}{3\sqrt{3}} \frac{K_1}{M_{\mathrm{S}}^1} \frac{\pi \gamma_{\mathrm{w}}}{\delta_{\mathrm{w}}} \left(\frac{A^1}{A^2} - \frac{K_{\mathrm{u}}^2}{K_{\mathrm{u}}^1} \right), \tag{1}$$

where M_{S}^1, A^1 (A^2), and K_{u}^1 (K_{u}^2) are the saturation magnetization, exchange stiffness parameter, and uniaxial anisotropy constant, respectively, and where the superscript 1 represents the particles and the superscript 2 represents the GB. In a hard magnet, the DW depins from the GB while maintaining its structure because the hard magnet has uniaxial anisotropy. Therefore, the depinning mechanism of the DW at the GB is easy to understand analytically, and theoretical analysis based on Eq. (1) can explain the experimental results.[10–17] However, studies of the depinning mechanism in soft magnets have been reported using measurements and analysis of the coercive force with a composite material, which is made using a hard magnet and α-Fe at particles and the GB.[13,14,18,19] In other studies, measurements of the magnetization curve have been shown.[6,7] However, the analytical equation of the DW depinning field in soft magnets is not well understood.

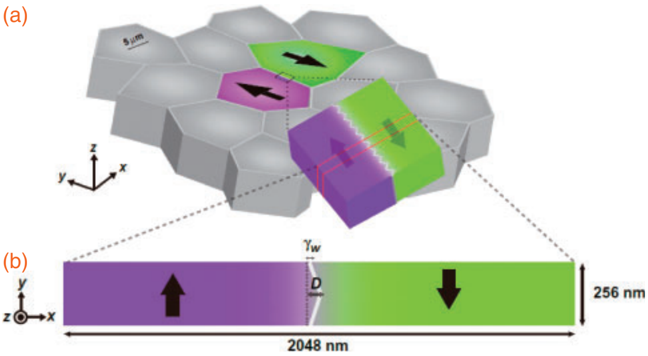

Fig. 1. (a) Model of a soft magnet. (b) Model of a micromagnetic configuration of a magnet that has a lateral size of $2048 \times 256\,\mathrm{nm}^2$ in the x–y direction. In the z-axis direction, the film is sufficiently thick. The white color indicates a grain boundary with a roughness (depth) of the misaligned GB (D) with the GB width $\gamma_{\mathrm{w}} = 4\,\mathrm{nm}$.

In this work, we investigated the DW depinning mechanism at the GB in an iron-based soft magnet using micromagnetic simulations. We examined the DW pinning from the GB by changing the GB roughness. The results showed that the 90° DW is pinned at the GB, and that 90° DWs are depinned successively in different magnetic fields. The DW depinning field decreases with increasing GB roughness. This is because the amount of DW energy at the GB is reduced by decreasing the pinning area of the 90° DW with increasing GB roughness. Additionally, we examined the overlapping area of the DW energy distribution and the GB, and derived analytically the empirical equation of the DW depinning field with the misaligned GB.

In the simulations, the motion of the magnetization in the wire was calculated using the Landau–Lifshitz–Gilbert equation.[20] We focused on the GB between particles as shown in Fig. 1(a), and determined that the lateral size of the magnet was $2048 \times 256\,\mathrm{nm}^2$ in the x–y direction, as shown in Fig. 1(b). In the z-axis, the film was sufficiently thick, and the calculated cell size was $2 \times 2\,\mathrm{nm}^2$. The GB width ($\gamma_{\mathrm{w}}$) was 4 nm, as shown in white in Fig. 1(b). The GB was assumed to have a bent structure from the center position of the GB, and the roughness (depth) of the misaligned GB was denoted as D. The boundary conditions of the $x(y)$-axis direction in the calculations were the fixed (periodic) boundary.

Typical material parameters for the soft magnet of 6.5 wt% Si–Fe were used. For the particles (superscript 1), $M_{\mathrm{S}}^1 = 1.62$ kemu/cm^3, $A^1 = 1.0\,\mu$erg/cm, the Gilbert damping constant

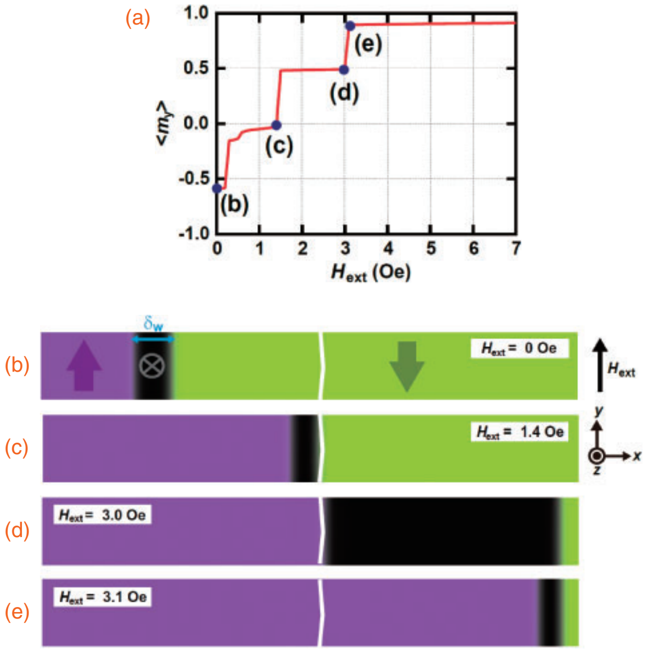

Fig. 2. DW depinning mechanism for $D = 80$ nm. (a) Results of the average magnetization in y-axis direction, $\langle m_y \rangle$, when the DW is pinned and depinned from the GB by H_{ext}. H^{depin} is 3.1 Oe. (b)–(d) Snapshots of the DW motion. The GB is shown in white. (b) The DW is located at the initial position. δ_w is the DW width. (c) The DW is pinned at the GB. (d) The left 90° DW is pinned at the GB. (e) The left 90° DW is depinned.

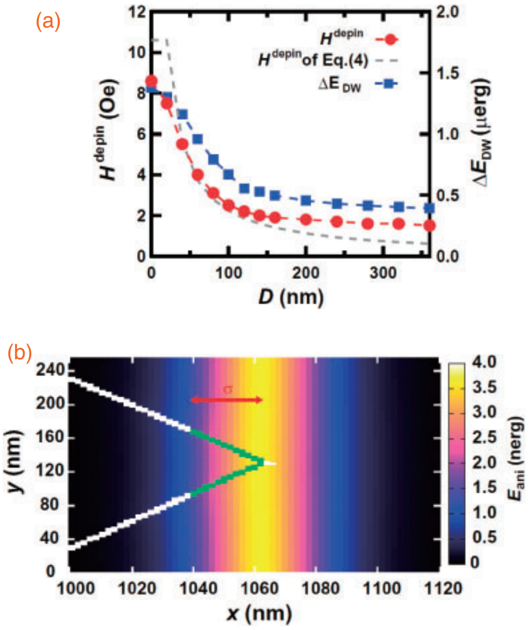

Fig. 3. (a) Effect of D on H^{depin} (red dots), ΔE_{DW} (blue dots), and theoretical values from Eq. (4) (dotted lines). (b) E_{ani} of DW energy at GB for $D = 80$ nm. The GB indicates white and green regions where E_{ani} is zero. The green region shows the overlapping area (σ) of E_{ani} with the GB.

$\alpha^1 = 1.0$, and the magnetocrystalline anisotropy constant $K_c^1 = 0.362$ Merg/cm^3. For the GB (superscript 2), M_S^2, A^2, and α^2 had the same values as those of the particles, and $K_c^2 = 0$ erg/cm^3. We assumed that K_c^2 is zero because this makes the analysis easier when we want to understand the DW depinning mechanisms. The magnetostriction was ignored. No nucleation mechanism from either the particles or the GB was introduced. The external magnetic field (H_{ext}) was applied in the y-axis direction.

Figure 2 shows the DW depinning mechanism for $D = 80$ nm. In Fig. 2(a), the results show the value of the average magnetization in the y-axis when the DW is pinned and depinned from the GB by H_{ext}. Figures 2(b)–2(e) show snapshots of the DW motion caused by H_{ext}. Figure 2(b) shows the initial DW position. Here, the DW width δ_w is 202 nm. The DW moves with H_{ext}, and the right 90° DW is pinned at the GB. It stays pinned at the GB until $H_{ext} = 1.4$ Oe, and then the DW shrinks to $\delta_w \sim 167$ nm [Fig. 2(c)]. The right 90° DW is then depinned from the GB at $H_{ext} = 1.5$ Oe, and spreads to the right edge of the calculation region.

The left 90° DW is pinned at the GB until $H_{ext} = 3.0$ Oe, as shown in Fig. 2(d). Finally, the left 90° DW is depinned from the GB at $H_{ext} = 3.1$ Oe [Fig. 2(e)]. This external field is defined as the DW depinning field (H^{depin}). In this way, the right and left 90° DWs are pinned at the GB, and they are depinned from the GB at different magnetic fields. Here, the 90° DW width (δ_w^{90}) does not change regardless of the DW pinning and depinning; however, it is changed by up to 4% from the initial width with $\delta_w^{90} \sim 55.0$ nm. The DW width does not change depending on D.

The effect of D ($D = 0$–360 nm) on H^{depin} is shown in red points in Fig. 3(a). H^{depin} sharply decreased below $D \sim 100$ nm. Then, H^{depin} gradually decreased with increasing D. The results show that H^{depin} decreased with increasing roughness of the misaligned GB. To understand this phenomenon, we investigated the change in the DW energy when the DW is pinned and depinned at the GB. The DW energy (E_{DW}) was obtained from the following equation:

$$E_{DW} = E_{exch} + E_{ani} + E_{demag}, \tag{2}$$

where E_{exch}, E_{ani}, and E_{demag} are the exchange energy, magnetocrystalline anisotropy energy, and demagnetization energy, respectively. The energy barrier (ΔE_{DW}) was obtained from the difference in E_{DW} before and after the DW is depinned ($\Delta E_{DW} = E_{DW}^{depin} - E_{DW}^{pin}$). The change in the ΔE_{DW} with D is shown in the blue points in Fig. 3(a). The results are in good agreement with the change in H^{depin} (red points) and show that E_{DW} decreased with increasing D.

To understand the relationship between the change in E_{DW} and the shape of the GB analytically, we investigated E_{DW} just before the DW is depinned. E_{ani} is shown in Fig. 3(b) just before the left 90° DW is depinned from the GB [Fig. 2(d)]. E_{ani} is zero in the GB, as indicated by white and green regions. The difference in E_{exch} is small because the exchange stiffness parameter (A) does not change between the particles and the GB. Additionally, E_{demag} is one order of magnitude smaller than E_{ani} and E_{exch}. The center of the left 90° DW is pinned at the GB edge, and E_{ani} has a normal distribution with a standard deviation of $\sigma = 23$ nm around the GB edge. Here, it is defined as the overlapping area (S_1: green region) where σ overlaps with the GB. The overlapping area for $D = 0$ is S_0, and the ratio of the overlapping areas S' ($= S_1/S_0$) is determined. S' is obtained using similar triangles as described below:

$$S' = \frac{1}{2D}(2\sigma - \gamma_w). \tag{3}$$

We extended Eq. (1), which led to the following empirical equation by considering S':

$$H^{\mathrm{depin}} = \frac{2}{3\sqrt{3}} \frac{K_1}{M_{\mathrm{S}}^1} \frac{\pi \gamma_{\mathrm{w}}}{\delta'_{\mathrm{w}}} S' \left(\frac{A^1}{A^2} - \frac{K_{\mathrm{u}}^2}{K_{\mathrm{u}}^1} \right), \tag{4}$$

where the DW width (δ'_{w}) of Eq. (4) is the twice the width of the 90° DW just before it is depinned ($\delta'_{\mathrm{w}} = 2\delta_{\mathrm{w}}^{90} \sim 111.2$ nm). This is consistent with the case of the half DW width in Ref. 10. When $D = 80$ nm, H^{depin} is 2.8 Oe, which was derived from Eq. (4) with $S' \sim 0.26$ obtained from Eq. (3). From Eqs. (3) and (4), the analytical results of H^{depin} are shown by dotted lines in Fig. 3(a), where S' is equal to 1 in the case of $D < 23$ nm because the GB is present in the σ of the E_{ani} distribution. The H^{depin} obtained using Eq. (4) decreased with increasing D, and is in good agreement with the calculated H^{depin} values.

There is a discrepancy in H^{depin} between the simulations and the analysis in the case of small D because the 90° DW is not pinned at the center position of the GB. In the case of large D, because the 90° DW is pinned at a position where it is not dependent on D, H^{depin} is almost unchanged in the simulations.

We investigated the DW depinning field and mechanisms in an iron-based soft magnet with a misaligned GB using micromagnetic simulations. The DW is pinned at the GB, and the 90° DWs are successively depinned with different magnetic fields. H^{depin} decreased with increasing GB roughness (D). H^{depin} decreased because the overlapping areas of the DW to the GB decreased with increasing D. At the same time, the amount of DW energy also decreased. We examined the ratio of the overlapping area with the DW energy and the GB, and derived an empirical equation of H^{depin} with the misaligned GB. The results obtained in this work not only clarify the underlying physics of the DW depinning mechanism but also pave the way to designing soft magnets to decrease coercive force.

Acknowledgments This work was supported by the Japan Society for the Promotion of Science (JSPS) KAKENHI Grant Number 2639008. KY was supported by the JSPS Postdoctoral Fellowships for Research.

1) Y. Yoshizawa, S. Oguma, and K. Yamauchi, J. Appl. Phys. **64**, 6044 (1988).
2) K. Suzuki, A. Inoue, and T. Masumoto, J. Appl. Phys. **70**, 6232 (1991).
3) M. A. Willard, D. E. Laughlin, M. E. McHenry, D. Thoma, K. Sickafus, J. O. Cross, and V. G. Harris, J. Appl. Phys. **84**, 6773 (1998).
4) A. Makino, H. Men, T. Kubota, K. Yubuta, and A. Inoue, Mater. Trans. **50**, 204 (2009).
5) A. Makino, IEEE Trans. Magn. **48**, 1331 (2012).
6) C. Kaido, T. Abe, Y. Okazaki, S. Kitahara, H. Yokota, A. Aoki, and K. Hosoyama, J. Magn. Soc. Jpn. **20**, 649 (1996) [in Japanese].
7) C. Kaido, Denki Gakkai Ronbunshi A **131**, 466 (2011) [in Japanese].
8) Y. Tanaka, Y. Takada, M. Abe, and S. Masuda, J. Magn. Magn. Mater. **83**, 375 (1990).
9) K. N. Kim, L. M. Pan, J. P. Lin, Y. L. Wang, Z. Lin, and G. L. Chen, J. Magn. Magn. Mater. **277**, 331 (2004).
10) R. Friedberg and D. J. Paul, Phys. Rev. Lett. **34**, 1234 (1975).
11) H.-R. Hilzinger and H. Kronmüller, Phys. Lett. A **51**, 59 (1975).
12) H. Kronmüller, K.-D. Durst, and M. Sagawa, J. Magn. Magn. Mater. **74**, 291 (1988).
13) T. Schrefl, J. Fidler, and H. Kronmüller, Phys. Rev. B **49**, 6100 (1994).
14) H. Kronmüller, R. Fischer, M. Seeger, and A. Zen, J. Phys. D **29**, 2274 (1996).
15) H. Kronmüller, R. Fischer, R. Hertel, and T. Leineweber, J. Magn. Magn. Mater. **175**, 177 (1997).
16) T. Schrefl, R. Fischer, J. Fidler, and H. Kronmüller, J. Appl. Phys. **76**, 7053 (1994).
17) H. Kronmüller and D. Goll, Physica B **319**, 122 (2002).
18) R. Fischer, T. Leineweber, and H. Kronmüller, Phys. Rev. B **57**, 10723 (1998).
19) N. M. Saiden, T. Schrefl, H. A. Davies, and G. Hrkac, J. Magn. Magn. Mater. **365**, 45 (2014).
20) Y. Nakatani, Y. Uesaka, and N. Hayashi, Jpn. J. Appl. Phys. **28**, 2485 (1989).